Numerical simulations of internal flow fields in a nozzle with liquid fertilizer deep machinery

Jihua Yang [a], Fanke Kong [b]

Yantai Research Institute, China Agricultural University Yantai, Yantai, China

[a] 1226054701@qq.com, [b] kfk2000@sina.com

Abstract. Fertilizing with water jet is a non-contact fertilization technique that uses high pressure water jet for hole-caving and fertilizing. In this article, an automatic liquid fertilizer deep machinery is proposed. The influences of three typical nozzles on the liquid fertilizer deep machinery were investigated via numerical simulations. The feasible water jet nozzle structures were obtained based on analysis and optimization of the main flaws of the four nozzles. A three-dimensional mathematical model of internal flow field in a high-pressure nozzle was established using the ANSYS software. Using the standard k-ε turbulent model, the internal flow field in the nozzle was simulated and the influences of nozzle parameters on the flow rate isogram and axial flow rate at the outlet of the flow field were studied. The results revealed that the axial flow rate at the outlet increased and then decreased as the convergence angle increased. The effects of cylinder section length on the axial flow rate at the outlet were negligible within a certain range. As the outlet diameter increased, the axial flow rate at the outlet decreased.

Keywords: water jet, liquid fertilizer deep machinery, nozzle, internal flow field conceptual design, numerical simulation.

1. Introduction

At present, the production and use of international liquid fertilizer are mainly concentrated in North America and Europe, accounting for about 70% of the world's total use, and about 25% in Western Europe.

Some developing countries (such as China and India) are also vigorously promoting it. Particularly, deep application of liquid fertilizer is an important technology of dry farming technology. Thus, water-saving agriculture technologies such as drought-resistant fertilizing have attracted increasing attentions recently. A typical drought-resistant fertilizing technique is deep application technology of liquid fertilizer. Over the past decade, considerable efforts have been made in studies of deep application technology of liquid fertilizer and relevant systematic designs in the world. Researchers from China Agricultural University et al. investigated the soil infiltration of irrigation water in deep application technology of liquid fertilizer and proposed an infiltration model. Northwest A&F University et al. investigated the unit load capacity, the water tank capacity and the water supply in in-row watering; equations for estimation of unit load capacity and water supply were proposed. Inner Mongolia Agricultural University et al. reported a study of water-saving principles of deficient irrigations, soil infiltration of local irrigation water, distributions and variations of water in the soil, cultivation resistance of ditching components, and accelerated water/soil mixing. The segregation homogeneity of the water segregator was also investigated. These studies serve as good references for design and development of walking-type water-saving irrigation units and water- fertilizing units. Nevertheless, application of mechanized deep application technology of liquid fertilizer is limited by various issues, including incompatibility with on-film bunch plating and no-tillage fertilizing, varying quantity of irrigation water, challenges in synchronized fertilizing, water splashing and poor understanding of the water infiltration process. Additionally, large energy dissipation and significant variations in depths and inter-bunch distances were also frequently observed in mechanized ditching. Therefore, fundamental and systematic studies of deep application technology of liquid fertilizer techniques are urgently needed.

At present, there are three types of liquid fertilizer machines commonly used: foliar fertilizer spraying liquid fertilizer equipment, liquid fertilizer drip irrigation equipment and liquid fertilizer sowing and application machinery. Liquid fertilizer sowing and application machinery can be divided into hanging liquid ammonia fertilization machinery, traction liquid fertilizer fertilization machinery and assembled liquid fertilizer fertilization machinery. The suspended liquid fertilizer fertilization machine has the advantages of simple structure, easy disassembly and assembly and stable operation. It is most widely used and popularized in China. The existing fertilizing machinery in the world has a working width of 19.8m and is equipped with 400 horsepower tractors with an operating efficiency of 16 hectares per hour. At present, there are hand-held fertilizer gun, pin-type liquid fertilizer deep machine driven by crank connecting rod mechanism, variable sprayer and so on in liquid fertilizer application machinery in China market. The disc liquid fertilizer deep hole planter is a new high-efficiency liquid fertilizer application machine developed to meet the requirements of liquid fertilizer deep sowing and high-speed operation.

In this article, we propose a novel liquid fertilizer deep machinery (see Figure 1) consisting of a water tank, a frame, a high-pressure axis tube, a jet wheel disc, a jet nozzle, and a duckbill pipe. Pressurized water in the high-pressure axis tube was ejected towards the soil once the high-pressure axis tube outlet is aligned with the jet nozzle (the jet wheel disc is vertical to the ground). In this way, hole-caving is achieved. Meanwhile, seeds are accurately thrown in the hole. The duckbill pipe can achieve self-moving and eliminate straws and weeds to facilitate hole-caving. This fertilizing approach is a promising one as it simplifies the fertilizing process and achieves water saving and conservation agriculture. Herein, the design of structural and performance parameters plays a key role.

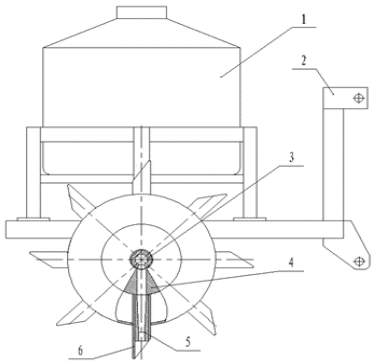


Figure 1. Schematic of the liquid fertilizer deep machinery proposed (1. water tank 2. frame 3. high-pressure axis tube 4. jet wheel disc 5. jet nozzle 6. duckbill pipe)

The principles of soil infiltration in high-pressure water jet fertilizing have not been fully understood as soil is a porous multi-phase medium. One-dimensional theories are not capable of predicting the jet nozzle and rheological behaviors of the water jet, while experimental studies are limited by model size, flow disturbance and poor accuracy. Since the 1980s, computational fluid dynamics (CFD) has been widely used for multi-dimensional numerical simulations of the water jet and the jet nozzle, owing to its advantages in accuracy, reliability and efficiency. Numerical simulations of the internal fields in the nozzle of the liquid fertilizer deep machinery proposed were achieved using FLOTRAN CFD, ANSYS. The effects of nozzle structural parameters on the jet velocity at the outlet were investigated and optimization of these parameters was achieved. This study provides a good reference for future studies of hole-caving by water jet in fertilizing.

2. Structural parameters of nozzle in the liquid fertilizer deep machinery

In virtue of advantages such as low resistance, high flow rate and large flow coefficients, facile manufacturing and cost-effectiveness, converging conical nozzles are regarded as ideal candidates for liquid fertilizer deep machinery s. As shown in Figure 2, key structural parameters involved were the nozzle convergence angle (α), the inlet diameter (D), the outlet diameter (d), the nozzle length (L) and the length of the cylinder at the nozzle outlet (S). These parameters have a significant effect on

the discharge velocity of the jet, thus affecting the hole-caving performance of the seeder. As the discharge velocity increases, the jet impact increases and the hole-caving performance of the seeder is improved.

3. Modelling

3.1. Physical model

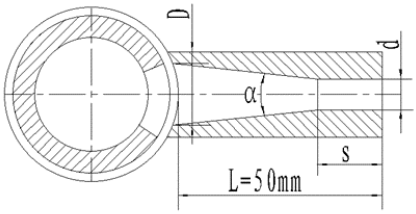


Figure 2. Schematic illustration of the jet nozzle flow Passage.

Figure 2 shows the physical model of the jet nozzle flow passage. Assuming L = 50 mm, D can be determined once L, S, α and d were determined; assume that the medium in the nozzle is incompressible water in turbulent motion. The effects of S, α and d on the internal flow field of the nozzle were investigated.

3.2. Governing equations

As the flow in the converging conical nozzle is a turbulent one, continuity equations and Navier-Stokes equations were employed as the governing equations and closed governing equations were established using a k-ε double equation turbulence model.

The continuity equations of incompressible fluids in Cartesian coordinates are as follows:

$$\frac{\partial v_x}{\partial x}+\frac{\partial v_y}{\partial y}+\frac{\partial v_z}{\partial z}=0 \tag{1}$$

The Navier-Stokes equations of incompressible fluids in Cartesian coordinates are as follows:

$$X-\frac{1}{\rho}\frac{\partial p}{\partial x}+\eta\left(\frac{\partial^2 v_x}{\partial x^2}+\frac{\partial^2 v_y}{\partial y^2}+\frac{\partial^2 v_z}{\partial z^2}\right)=\frac{dv_x}{dt} \tag{2}$$

$$Y-\frac{1}{\rho}\frac{\partial p}{\partial y}+\eta\left(\frac{\partial^2 v_x}{\partial x^2}+\frac{\partial^2 v_y}{\partial y^2}+\frac{\partial^2 v_z}{\partial z^2}\right)=\frac{dv_y}{dt} \tag{3}$$

$$Z-\frac{1}{\rho}\frac{\partial p}{\partial z}+\eta\left(\frac{\partial^2 v_x}{\partial x^2}+\frac{\partial^2 v_y}{\partial y^2}+\frac{\partial^2 v_z}{\partial z^2}\right)=\frac{dv_z}{dt} \tag{4}$$

The turbulence kinetic energy (k) and dissipation rate (ε) of the k-ε double equation turbulence model can be described by:

$$\frac{\partial(\rho k)}{\partial t}+\frac{\partial(\rho k u_i)}{\partial x_i}=\frac{\partial}{\partial x_j}\left[\left(\mu+\frac{\mu_i}{\sigma_k}\right)\frac{\partial k}{\partial x_j}\right]+G_k+G_b-\rho\varepsilon-Y_M+S_k \tag{5}$$

$$\frac{\partial(\rho\varepsilon)}{\partial t}+\frac{\partial(\rho\varepsilon u_i)}{\partial x_i}=\frac{\partial}{\partial x_j}\left[\left(\mu+\frac{\mu_t}{\sigma_\varepsilon}\right)\frac{\partial \varepsilon}{\partial x_j}\right]+C_{1\varepsilon}\frac{\varepsilon}{k}\left(G_k+C_{3\varepsilon}G_b\right)-C_{2\varepsilon}\rho\frac{\varepsilon^2}{k}+S_\varepsilon \tag{6}$$

where G_k denotes the turbulence kinetic energy attributed to the gradients of average flow rate, G_b denotes the turbulence kinetic energy attributed to the buoyancy, and Y_M denotes the effects of compressible turbulent fluctuations on the overall dissipation rate.

The viscosity coefficient of the turbulence can be obtained by:

$$\mu_t=\rho C_\mu\frac{k^2}{\varepsilon} \tag{7}$$

For simulations using ANSYS, default constants were assumed as $C_{1\varepsilon}$=1.44, $C_{2\varepsilon}$=1.92 and $C_{3\varepsilon}$=0.09, the turbulence energy and the turbulence Prandtl Number of the dissipation rate (ε) were σ_k=1.0 and σ_ε=1.3.

3.3. Boundary conditions

The jet speed at the inlet can be obtained by V = Q/A. The results revealed that the optimized jet quantity was 0.08L. The initial travelling speed and inter-plant distance were 1 m/s and 200 mm, respectively. The wheel disc was equipped with eight nozzles and D=522 mm. According to tests it can be completed punching with water jet within the range of 1/2 plant spacing, The flow of each nozzle (Q) is 0.08L×60/(0.1) = 48 L/min and the relative static pressure at the outlet was negligible. The medium in all cases was water (density =1000 kg/m^3, viscosity = 1.004×10-6 m^2/s). The inner wall of the nozzle was solid boundaries.

3.4. Grid generation

Nozzle models were established using different parameter values. 2DFluent141 was selected as the system unit in ANSYS and the mesh size = 0.0002. The grid was generated by mapping division and the nozzle grid established is shown in Figure3.

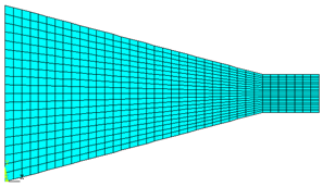
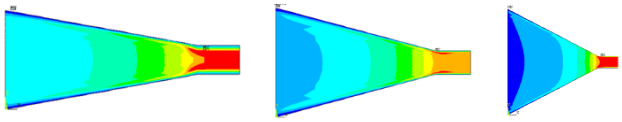


Figure 3. Schematic of the nozzle grid.

4. Results and discussions

4.1. Effects of α on the internal flow fields of the nozzle

Assuming S = 12 mm and d = 8 mm, the effects of α on the internal flow field of the nozzle were investigated using numerical simulations. Figure 4 illustrates the distributions of internal flow rate in the nozzle and Figure 6 shows axial flow rate at the outlet vs. α. As shown in Figure 5, the axial flow rate increased from inside outwards, and the parabolic isograms were symmetrical about the axis. A thin boundary layer was observed on the inner wall close to the nozzle. As shown in Figure 5, the axial flow rate at the outlet increased and then decreased as the convergence angle increased. At α = 30°, the axial flow rate at the outlet was maximized (17.5 m/s). At low convergence angles, the axial velocities at the inlet increased with α due to the limited cross-section area. Due to the cumulative action effect of the converging nozzle, the axial flow rate at the outlet increased with α. As α increased further, the axial velocities at the inlet decreased and the axial flow rate at the outlet decreased once it exceeds the Munroe effect. Hence, the optimized convergence angle is 30° in this case.



α=20° *α*=30° α=60°

Figure 4. Distributions of internal flow rate in the nozzle at different α.

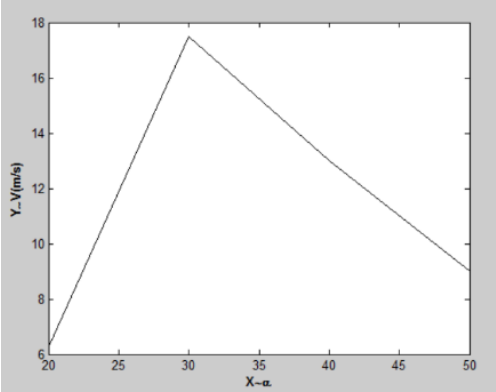
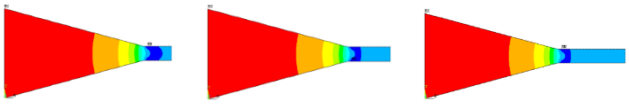


Figure 5. Axial flow rate at the outlet vs. α.

4.2. Effects of S on the axial flow rate at the outlet

Assuming α = 30° and d = 8 mm, the effects of S on the internal flow field of the nozzle were investigated using numerical simulations. Figure 7 illustrates the distributions of internal flow rate in the nozzle. The distributions of internal flow pressure in the nozzle also simulation. As shown in Figure 6, at a constant axial flow rate at the inlet, the parabolic internal flow rate is ogram was also symmetrical about the axis and the axial flow rate at the outlet was maximized. However, the axial flow rate at the outlet didn't show significant variations, indicating that the effect of S on the axial flow rate at the outlet is negligible. Although the flow resistance increased with S, the energy gathering process was achieved at the convergence section. The effect of S on the internal flow pressure in the nozzle was negligible. The internal flow pressure decreased along the axis and then stayed constant; a negative pressure area was observed at the junction of the convergence section and the cylinder. The cavitation phenomena, which would be observed once the pressure dropped below the local saturated vapor pressure, may reinforce the impact of water jet. Therefore, the presence of a negative pressure area facilitates the hole-caving process by water jet. The optimized length of the cylinder at the nozzle outlet is 15 mm in this case.



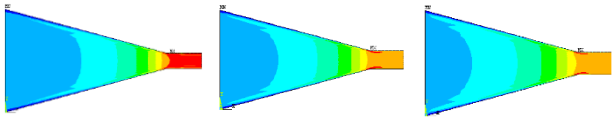
S=10mm S=15mm S=20mm

Figure 6. Distributions of internal flow rate in the nozzle at different S.

4.3. Effects of S on the axial flow rate at the outlet

Assuming α = 30° and S = 15 mm, the effects of d on the internal flow field of the nozzle were investigated using numerical simulations and the results are shown in Figure 7. As d increased, the axial flow rate at the outlet and the impact of the water jet decreased, while the discharge flow increased. As a result, the hole-caving process was facilitated. Additionally, the manufacturing cost increased as d decreased due to the increasing manufacturing precision. Therefore, the optimized outlet diameter is 10 mm in this case.

Parameter values are shown in Table 1. Based on results mentioned above, optimize



d=8mm d=10mm d=12mm

Figure 7. Distributions of internal flow rate in the nozzle at different

Table 1. Optimized structural parameters of the nozzle.

Structural Parameter	Convergence angle (α, °)	*Outlet diameter (d, mm)*	*Nozzle length (L, mm)*	*Length of outlet cylinder (S, mm)*	*Inlet diameter (D, mm)*
Value	30	10	50	15	28

4.4. The tests equipment and analysis

The tests equipment is showed as figure 8. The test parameters which the pressure, the throttle opening and the rotating speeds were 0.3MPa, 50% and 32 r/min (corresponding velocity is 1m/s). The jet nozzel structural parameters as table 1 in this study were: α = 30°, d = 10 mm, L = 50 mm, S = 15 and D = 28 mm. Thus the liquid fertilizer deep machinery can meet the design requirements. The experiment showed that the axial flow rate at the outlet was 16.7 m/s, is the theoretical value 95%. This study can provides reference for liquid fertilizer deep fertilization machine and liquid fertilizer deep machinery.



Figure 8. The diagram of test equipment

5. Conclusions

5.1. Numerical simulations of the internal

Fields in the nozzle of the liquid fertilizer deep machinery proposed were achieved using FLOTRAN CFD, ANSYS. The effects of nozzle structural parameters on the jet velocity at the outlet were investigated and optimization of these parameters was achieved. This study provides a good reference for future studies of hole-caving by water jet in fertilizing.

5.2. Key structural parameters of the nozzle

Include the nozzle convergence angle, the inlet diameter, the outlet diameter, the nozzle length and the length of the cylinder at the nozzle outlet. Optimization of these parameters is of great significance for water jet fertilizing.

As α increased, the axial flow rate at the outlet increased and then decreased. The effects of cylinder section length on the axial flow rate at the outlet were negligible within a certain range. As the d increased, the axial flow rate at the outlet decreased.

5.3. The optimized values of key structural

Parameters of the nozzle determined in this study were: α = 30°, d = 10 mm, L = 50 mm, S = 15 and D = 28 mm.

Acknowledgment

The research was supported by the scientific research Fund of National Natural Science Foundation of China (51711520319).

References

[1] Chen Yuanyuan, You Jiong, Xing Zefeng, et al. Review of precision agriculture development situations in the main countries in the world and suggestions for China[J]. Transactions of the Chinese Society of Agricultural Engineering (Transactions of the CSAE), 2021, 37(11): 315-324. (in Chinese with English abstract)

[2] Wang Xiaoshan, Yan Haijun, Zhou Lingjiu, et al. Experimental research of hydraulic performance on jet fertilizer applicator of SSQ series[J]. Transactions of the Chinese Society of Agricultural Engineering (Transactions of the CSAE), 2020, 36(21): 31-38. (in Chinese with English abstract)

[3] Li H, Liu Y, Cai J B, Mao X M. Change of sap flow rate and stem diameter microvariation of summer maize and influence factors. Transactions of the CSAE, 2011; 27(10): 187–191. (in Chinese with English abstract)

[4] Bao Z, Wu W Y, Liu H L, Hao Z Y, Niu Y. Response of Environmental Factors and Characteristics of Variation on Muskmelon Sap Flow with Mulched Drip Irrigation in the Solar Greenhouse. Chinese Agricultural Science Bulletin, 2012; 28(28): 140–147. (in Chinese with English abstract)

[5] James S A, Clearwater M J, Meinzer F C, Goldstein G. Heat dissipation sensors of variable length for the measurement of sap flow in trees with deep sapwood. Tree Physiology, 2002; 22(4): 277–283

[6] Huang Lihua, Shen Genxiang, Qian Xiaoyong, et al. Impacts of drip fertilizer irrigation on nitrogen use efficiency and total nitrogen loss load. Transactions of the Chinese Society of Agricultural Engineering (Transactions of the CSAE), 2008, 24(7): 49 − 53.(in Chinese with English abstract)

[7] Neilsen D, Parchomchuk P, Nelsen G H, et al. Using soil solution monitoring to determine the effects of irrigation management and fertigation on nitrogen availability in high-density apple orchards. Journal of the American Society for Horticultural Science, 2005, 123(4): 706 − 713

[8] Ayars J E, Phene C J, Hutmacher R B, et al. Subsurface drip irrigation of row crops: A review of 15 years of research at the water management research laboratory. Agricultural Water Management, 1999, 42(1): 1 − 27

[9] Hartz T K, Hochmuth G J. Fertility management of drip irrigated vegetables. Hort Technology, 1996, 6(3): 168 − 172

[10] Li Jiusheng, Du Zhenhua, Li Yanfeng. Field evaluation of fertigation uniformity for subsurface drip irrigation systems. Transactions of the Chinese Society of Agricultural Engineering (Transactions of the CSAE), 2008, 24(4): 83 − 87. (in Chinese with English abstract)

[11] Xie Guanghui, Han Dongqian, Wang Xiaoyu, et al. Harvest index and residue factor of cereal crops in China. Journal of China Agricultural University, 2011, 16(1): 1 − 8. (in Chinese with English abstract)

[12] Oweis T Y, Farahani H J, Hachum A Y. Evapotranspiration and water use of full and deficit irrigated cotton in the Mediterranean environment in northern Syria[J]. Agricultural Water Management, 2011, 98(8): 1239 − 1248

[13] Ierna A, Lombardo G P, Mauromicale G. Tuber yield, water and fertilizer productivity in early potato as affected by a combination of irrigation and fertilization[J]. Agricultural Water Management, 2011, 101(1): 35 − 41

[14] ShengFeng, ZhangLiyong and WuDan. Review on research theories and observation techniques for preferential flow in unsaturated soil[J]. Transactions of the Chinese Society of Agricultural Engineering (Transactions of the CSAE),2016,32(6):1-10.(in Chinese with English abstract)

[15] Yuan Jiwang, Zhu Delan, Gao Sasa, et al. Optimization of structural parameters and performance experiment of jet fertilizer injector based on numerical simulation[J]. Transactions of the Chinese Society of Agricultural Engineering (Transactions of the CSAE), 2021, 37(14): 52-59. (in Chinese with English abstract)

[16] Yu Changchang, Wang Qingjie, He Jin, Li Hongwen, Lu Caiyun, Liu Zhengdao. Development of spraying device for precise and deep application of liquid fertilizer in sowing period[J]. Transactions of the Chinese Society of Agricultural Engineering (Transactions of the CSAE), 2019, 35(16): 50 − 59. (in Chinese with English abstract)